CSP MODELING METHODOLOGY FOR MACRO DECISION MAKING - EMPHASIS ON THE CENTRAL RECEIVER TYPE

Paul Gauché[1], Theodor W. von Backström[2] and Alan C. Brent[3]

[1] MEng (Mech), Sr. Researcher and Coordinator STERG, Dept. Mechanical and Mechatronic Engineering, Stellenbosch University, Private Bag X1, Matieland, 7602, South Africa, Phone: +27 21 808 4242, E-Mail: paulgauche@sun.ac.za.

[2] PhD, Senior Researcher and Emeritus Professor, Dept. Mechanical and Mechatronic Engineering, Stellenbosch University.

[3] PhD, Professor of Sustainable Development, School of Public Leadership & Associate Director, Centre for Renewable and Sustainable Energy Studies, Stellenbosch University.

Abstract

Concentrating solar power (CSP) has been identified as a primary long term method of generating sustainable power in South Africa. In order to successfully achieve a large-scale rollout of CSP that is most affordable and whereby the domestic economy can participate most effectively, decisions need to be made as soon as possible. These decisions include: investments into R&D, education and training; investments in pilot plants; tariff levels; long term transmission grid planning; and many others.

As part of a larger study investigating the techno-economic prerequisites of a large-scale rollout, the objective of this work is to deliver a fast and simple method to evaluate CSP plant performance. These models will be used for regional planning scenarios later. This paper focuses on the optical-to-thermal conversion of energy in central receiver plants using a method simple enough to give near instantaneous results but detailed enough to be reasonably accurate. The result is a method that has passed initial validation for the optical-to-thermal conversion when compared against more sophisticated methods and measured results for the eSolar SierraTowers near Lancaster, CA. Further work is needed to find a suitable power block model that matches the needs of the project.

Keywords: Central receiver, optical, thermal, modeling for decision making

1. Introduction and background

Concentrating solar power (CSP) has been identified by key stakeholders as a significant, if not the primary [1] 21st century sustainable method of electricity production in South Africa. These stakeholders include international agencies such as the IEA [2], government, the private sector and research institutions. Amongst other activities, the South African Department of Science and Technology (DST) commissioned a Solar energy roadmap for South Africa in 2010 [3] in response to the commitments made by government to meet climate change targets while provisioning for the increasing needs of power for the nation. Fluri [4] reports that the potential for CSP in suitable areas within 20 km of the existing transmission lines of South Africa far exceeds the current capacity of the national utility, Eskom.

Thermal inertia and storage enables a CSP plant to deliver power when there is no direct sun. Recently a new CSP plant in Spain set a record of 24 continuous hours of electricity production and is developed to average 20 hours to the network per day [5]. When hybridized with backup fuel, CSP can feasibly deliver baseload electricity. CSP has also been identified as an opportunity for localization in South Africa with many parts of the plant potentially manufacturable in the country, particularly for the central receiver and linear Fresnel types.

Although the importance of CSP has been identified, there are several barriers at least to the initial uptake of the technology. CSP is relatively unknown in South Africa with no plants in operation and only very small prototypes demonstrated. CSP plants are commercially viable at larger scale, typically 50 MW per plant but the capital costs are high. The regulatory environment is in upheaval at the time of writing due to the

uncertainty regarding renewables and the lack of experience with renewable feed in tariffs (REFIT) [6]. These factors need to be addressed not only to change to sustainable power methods but also to provide a stable environment for lower cost financing and to initiate a new industry.

The urgency for short and long term electricity capacity in South Africa where rolling blackouts have occurred in recent years is compounded by the dependence on electricity from coal (above 90% of capacity). Some of the largest coal power plants ever built are now being constructed after about 15 years of adding almost no capacity. The National Energy Regulator of South Africa (NERSA) has approved price increases of about 25% per year starting 1 April, 2010, through 31 March, 2013. Eskom has indicated that similar increases of this magnitude are required until 2016 to balance the books [7]. If prices of conventional electricity continue to increase as planned by about 25% per year, and if the learning rate for CSP is between 10% and 15% as assumed in most publications, the LEC will reach parity before the end of this decade.

Moving forward, the promulgated (mandated) Integrated Resource Plan for the next 20 years (IRP 2010 – 2030) [8] includes 17.8 GW of renewables from wind, PV and CSP. The IRP is a new planning process devised to balance the needs of the country with the assumption of a significant role by independent power producers (IPPs) in the future. It recognizes major challenges that need to be balanced with care including poverty, water supply, climate change, transmission requirements, and natural and fuel resources. The IRP sets out the allocation of new capacity on an annual basis over 20 years and will be refreshed every two years based on new data.

In the short term, as the first CSP plants based on foreign technologies are constructed and brought into operation, the skills and knowledge base pertaining to CSP needs to grow rapidly in preparation for the intermediate to long term. It will be important to grow knowledge broadly and deeply in order to make effective decisions at the highest levels as well as to develop local economic opportunities through the development of intellectual property and industries. The purpose of this research is to develop tool to facilitate higher level decision making.

2. Objective

This paper specifically presents a method to evaluate the scale and performance of central receiver CSP plants with minimal user inputs and near instant results. This method is part of a CSP system modeling tool intended for quick plant analysis with the purpose of evaluating all CSP types using consistent boundary conditions and assumptions. It is being developed for fast analysis to provide the ability to scale up the use of the method to regional and national scenario planning. The system modeling tool in turn is part of a study to determine the techno-economic prerequisites to a large scale rollout of CSP in South Africa.

The research goal is to equip decision makers with a reasonable and impartial set of information and tools to plan for the following 40 years assuming that a large scale rollout will occur. The consequences of planning well for the large scale rollout are significant. The ability to start soon and establish a local CSP industry will potentially lead to a savings of over ZAR 200 billion [1] which in turn benefits from a multiplier effect due to localization.

2. Methodology

In short, this paper deals with the optical to power conversion of central receiver plants with an emphasis on the optical method. The model is developed and compared with published results for the eSolar pilot plant, the Sierra SunTower solar generating plant [9, 11]. Sensitivities to key plant parameters are then investigated. The focus on the optical component of the central receiver is driven by the detail required even in a simplified model as presented.

The model is a quasi-static hourly model using energy balances and efficiencies. The components of the plant incorporate irreversibilities such as explicit optical efficiency losses and real heat transfer, but are otherwise ideal. No distinction is made regarding specific heat transfer fluids or heat engines as this would not make sense for the macro objectives of the project. As such, the performance anchors to energy balance and

thermodynamic efficiencies based on reservoir temperatures. The solution is entirely analytical with no numerical iteration procedure for the optical or thermal components, making it stable and fast. The method is outlined briefly.

- Hourly solar and weather data over a typical mean year is used in combination with the position of the sun determined using standard approximations. Thus the DNI, solar azimuth and zenith angles are combined for each hour of the year.
- Necessary plant configurations are specified. This principally includes aperture, tower and power block sizing (in the case of the central receiver) with associated detail.
- Total heliostat field sizing is determined which then permits for the sizing of the receiver.
- Optical efficiency of the primary aperture is determined using a discretized lumped geometric approach. Cosine, blocking and shading losses are determined for every hour of the year.
- An energy balance is performed for the receiver and the energy output is then supplied to a simplified heat engine. Thermal inertia, storage and backup fuel are accounted for from an energy efficiency basis.
- The heat engine output is a function of both thermal energy availability and basic demand.

3. Optical approximation of the heliostat field and receiver

Numerical methods are preferred for the design and performance assessment of the optical sub-systems in a central receiver plant. These methods are computationally expensive and require attention to use and detail. Such a method was used in the design of the eSolar Sierra SunTowers [9]. As the objective of this work is not for design but for good enough information, an approximation method was considered sufficient. The method must however be capable of handling parametric scrutiny such that key parameters of these plants can be studied in more detail. The method uses only geometric approximations for the cosine, shading and blocking losses of heliostats. The rest of the plant model uses efficiency values and energy balance methods.

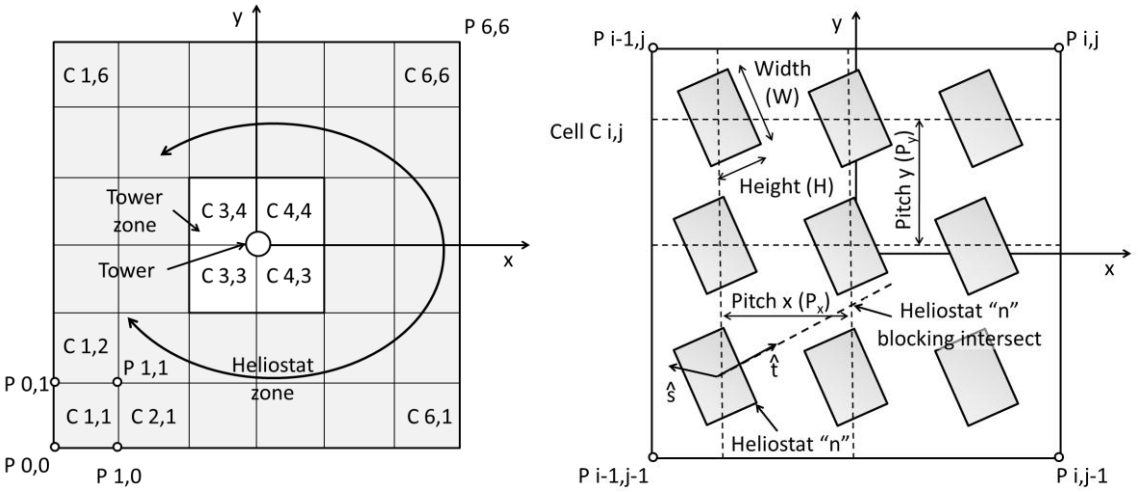

Fig. 1. Plan view of heliostat field zones and cells (left) and one heliostat cell (right)

The model divides the heliostat field into discrete zones per fig. 1. The field shown is rectangular with a tower zone in the center. The model is able to handle multiple configurations easily by weighting the cells between 0 and 1. In this way, the SierraTowers can be modeled by setting the weighting of the cells on the left and right of the tower zone to zero in order to represent the tower access road. Circular (or other) arrangements can be handled using the weighting method.

Each zone (or cell) has multiple heliostats but all heliostats in a cell are treated identically based on the center location of the cell. Fig. 1 on the right schematically shows the principle dimensions needed or produced in the analysis. The identical treatment of each heliostat is the key simplification in the model. The geometry of only 1 heliostat is determined and the impact of shading and blocking is done for heliostat "n" on itself. Then the entire cell is lumped into a macro heliostat for purposes of the whole field. In this way, the configuration

in fig. 1 shows only 32 macro heliostats (and 4 exclusion cells).

The geometric method determines the cosine (η_θ), blocking (η_b) and shading (η_s) efficiency of each cell. The simplest net hourly heliostat field optical efficiency (η_{oh}) is the product of the three terms and weighted for the entire field.

$$\eta_{oh} = \eta_\theta \, \eta_b \, \eta_s$$

A more accurate net heliostat field optical efficiency takes into account that shading and blocking tends to be mutually exclusive in their impact and so are additive losses. The combined shading and blocking is then multiplied by the cosine term to give the following.

$$\eta_{oh} = \eta_\theta \max(0, -1 + \eta_b + \eta_s)$$

A comparison shows only slight deviations at low solar altitudes and over a year the above efficiency formulations differ by 1.1% based on the case study. The annual combined efficiency used by Schell [10] is weighted by DNI for every hour (DNI_h) of the year giving the annual optical (cosine, shading and blocking) efficiency (η_o) as:

$$\eta_o = \frac{\sum_{t=1}^{8760}(\eta_{oh} DNI_h)}{\sum_{t=1}^{8760} DNI_h}$$

The net optical efficiency, sun-to-receiver is a product of the heliostat field efficiency (η_{oh}), heliostat availability (η_a), heliostat fouling (η_f), reflector specular reflectance (η_r) and receiver spillage efficiency (η_s). The latter is a function of reflector surface tolerance, tracking errors, calibration errors and wind. Due to the simplicity of the method, the receiver is sized linearly based on sun angle and the sum of angular errors, or if reduced in size, spillage incurs a linear efficiency penalty.

3.1. Cosine efficiency

The position of the sun and the receiver relative to the cell center determines the cosine efficiency. For convenience, Euclidean space is used to determine these relationships. Firstly, unit vectors (direction cosines) are determined from the cell center to the sun ($\hat{\boldsymbol{s}}$). This is the reverse direction of the radiation for convenience. The unit vector needs to be calculated for every hour of the year but is of course the same value for all cells.

The vertical (z) component is represented by the cosine of the zenith angle.

$$\hat{\boldsymbol{s}}_z = \cos(\theta_z)$$

The other two terms (x, y) are represented by the compliment of the vertical and the solar azimuth angle.

$$\hat{\boldsymbol{s}}_x = -\cos(\gamma_s)\, sin(\theta_z) \qquad \hat{\boldsymbol{s}}_y = -sin(\gamma_s)\sin(\theta_z)$$

Turning now to the reflected radiation unit vector ($\hat{\boldsymbol{t}}$), the direction of reflection will be unique for each heliostat but only needs to be determined once assuming that the image target does not move. In this way, the heliostat field will be represented with 32 reflection unit vectors as defined by the discrete heliostat cells in fig. 1 (left).

The norm of the cell to tower is given as

$$\|\boldsymbol{t}\| = \sqrt{\mathrm{T}^2 + {C_{\mathrm{i,j,x}}}^2 + {C_{\mathrm{i,j,y}}}^2}$$

where T is the tower height, $C_{\mathrm{i,j,x}}$ is the x position of a heliostat cell relative to the tower and $C_{\mathrm{i,j,y}}$ is the y position of a heliostat cell relative to the tower.

$$\hat{\boldsymbol{t}}_z = \frac{T}{\|\boldsymbol{t}\|} \qquad \hat{\boldsymbol{t}}_x = \frac{-C_{\mathrm{i,j,x}}}{\|\boldsymbol{t}\|} \qquad \hat{\boldsymbol{t}}_y = \frac{-C_{\mathrm{i,j,y}}}{\|\boldsymbol{t}\|}$$

Having defined the incident ($\hat{\boldsymbol{s}}$) and reflecting ($\hat{\boldsymbol{t}}$) unit vectors, the macro heliostat slope can be determined. Note that a slope is defined by a unit vector normal to a slope. We also know from basic optics that the angle

of incidence and reflection are the same. Also, the dot product of two unit vectors produces the cosine of the angle between them. This dot product angle represents twice the incidence angle on a heliostat.

$$\theta = \frac{\cos^{-1}(\hat{\boldsymbol{s}} \cdot \hat{\boldsymbol{t}})}{2}$$

This incidence angle (θ) is the angle used to determine the cosine efficiency of a heliostat (or any other aperture). The area (A) weighted sum of all macro heliostat cosines is the heliostat field cosine efficiency and is given by

$$\eta_\theta = \frac{\sum_{i,j=1}^{6} d \times A\, C_{i,j} \cos(\theta)}{\sum_{i,j=1}^{6} d \times A\, C_{i,j}}$$

where *d* is the heliostat weighting term for the heliostat field arrangement.

3.2. Shading and blocking efficiency

The heliostat shading and blocking efficiencies are based on the configuration shown in fig. 1 on the right. To satisfy the objectives of this project, a geometric approximation was developed to estimate the shading and blocking. This was achieved using primary geometric variables such as heliostat size and spacing, as well as the heliostat slope also determined for the cosine efficiency. The blocking and shading methods are the same with the exception of the unit vectors used. Succinctly, the blocking and shading methods utilize the reflected ($\hat{\boldsymbol{t}}$) and incident ($\hat{\boldsymbol{s}}$) unit vectors respectively and combine this with the geometry of the heliostats. The blocking method is described in some detail.

The first step involves determining which heliostats block the heliostat of interest. As this is a geometric approximation, the image blocked will not be accurately represented by shape, but will approximate the area blocked. Referring to fig. 1 (right), the reflecting heliostat "n" is blocked by the heliostat or heliostats at the intercept of the unit vector $\hat{\boldsymbol{t}}$ and the line representing a particular row or column of heliostats for a rectangular arranged set of heliostats. The method is easily modified to represent any arrangement of heliostats for which a pattern exists.

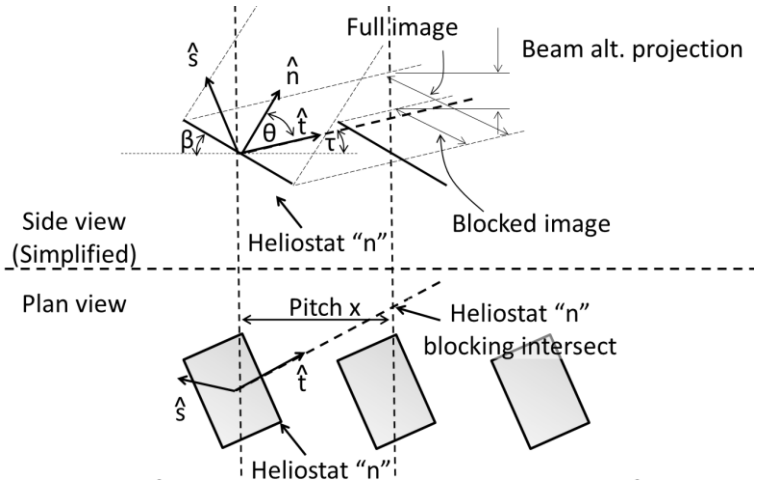

Fig. 2. Principle heliostat blocking parameters

Because a cell contains a group of heliostats, all heliostats in the cell assume the same direction vectors as a virtual heliostat at the center of the cell. The blocking and shading method described here is based on a heliostat "n" blocking and shading upon a copy of itself. The intercept is used only to determine the horizontally projected reflected light path length to the intercept and the elevation of the beam at the intercepting heliostat(s). For a rectangular array, if

$$\frac{|\hat{\boldsymbol{t}}_x|}{P_x} > \frac{|\hat{\boldsymbol{t}}_y|}{P_y}$$

then the blocking is caused by the heliostat row one line over in the x direction. Otherwise the blocking is caused by the adjacent heliostat row one line over in the y direction. It should be noted that for different arrangements, the logic of which heliostats cause the blocking will be different. For a circular arrangement, there will be no "if" statement. For the case where the above "if" test is true, the resultant "beam altitude projection" (B_a), the height of the image from the heliostat projected at the distance of the pitch of the intercepting heliostat(s) is defined as

$$B_a = \hat{\boldsymbol{t}}_z \frac{P_x}{|\hat{\boldsymbol{t}}_x|}$$

This value determines the vertical component of the non-blocked image. The equation is similar for the false "if" result. The blocking efficiency is a ratio of the reflection cosine of B_a to the angle of incidence cosine of the full image (see fig. 2) with a modification for the gaps between the blocking heliostats based on the ratio of the heliostat width (W) to pitch (P).

The blocking efficiency reduces to

$$\eta_b = \frac{B_a \cos(\tau)}{H \cos(\theta)} \times \frac{P}{W} = \frac{B_a \, \hat{\boldsymbol{t}}_z}{H \cos(\theta)} \times \frac{P}{W}$$

This simplified expression shows that maintaining a constant area but changing the dimensions (H, W) of a heliostat makes no difference to the result. This is a consequence of the simplification but is also perhaps indicative of the robustness of the method for its intended use.

The shading efficiency uses the same method but uses the incident unit vector instead of the reflected one.

$$\eta_s = \frac{B_a \, \hat{\mathbf{s}}_z}{H \cos(\theta)} \times \frac{P}{W}$$

3.3. Receiver energy balance

The optical energy delivered to the receiver each hour (E_{rih}) is determined by the solar absorptivity and efficiency terms listed earlier. A_c is the aperture area per cell and d is the cell weighting from before.

$$E_{rih} = DNI_h \propto_s \eta_f \, \eta_r \, \eta_a \, \eta_s \sum_{cells=1}^{n} (\eta_{ohc} d A_c)$$

An energy balance is calculated for an external receiver assuming a simple average receiver temperature where the receiver outlet temperature (T_r) is set to its rating assuming that flow rate will be controlled accordingly.

$$E_{rih} = \varepsilon_r A_r \left({T_r}^4 - {T_a}^4 \right) + h A_r (T_r - T_a) + E_{ro}$$

4. Results and discussion

Cosine, blocking and shading results are compared against the annual average value published by Schell [9] for the design of the SierraTowers plant. Thermal power delivered is determined and compared against experimental results also on the SierraTowers plant published by Meduri et al. [11]. Besides comparing with Lancaster in California (34.7° latitude) [12], results are also given for Upington, South Africa (-28.4° latitude). The model was adjusted to the SierraTower configuration by Schell [9]. An access road instead of a tower zone was set by a single row of cells. The number of cells was increased to 49 (7x7).

4.1. Cosine, shading and blocking efficiency

Schell [9] reports that the ray tracing algorithm predicts an annual efficiency of 70.1%. The tower height in the model is 50m. For the same configuration, the simplified model predicts 62.3% and 64.8% for Lancaster and Upington (South Africa) respectively. When the model is modified for a 55m tower per construction according to NREL and SolarPACES [13], the model predicts 67.2% and 69.9% respectively. Fig. 3 shows this efficiency as function of tower height. Per this result, a 55m tower is located near the inflection point where shading and blocking is no longer a significant factor in the performance of the plant.

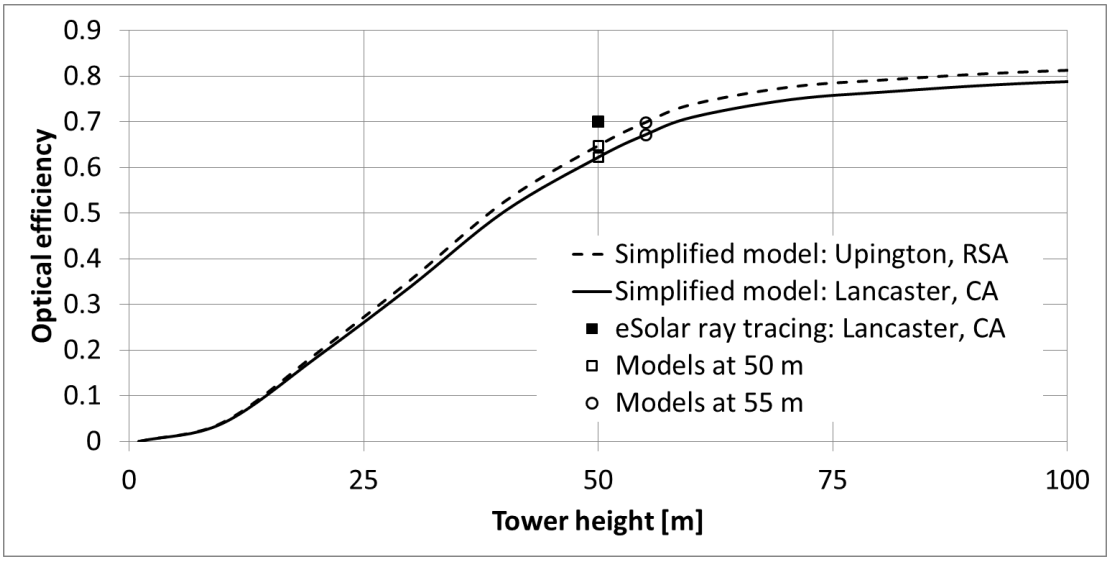

Fig. 3. Comparison of cosine, shading and blocking vs. tower height

4.2. Optical to thermal conversion

The quasi-steady thermal power result for the simplified model is compared with simulated and measured data published by Meduri et al. [11]. For the simplified model, the receiver was auto-sized for zero spillage (W = 2.9 m, H = 8.5 m), thus not based on actual receiver dimensions. Fouling and other optical losses were added to the heliostat field optical efficiency. An energy balance calculation was done based on a simple average receiver temperature and an outlet of 350°C. The solar absorptivity ($\propto_s$) was set to 0.85. A capacitance term is inserted between the energy delivered by the receiver and the power block to account for thermal inertia. Fig. 4 plots the result over a good midsummer day equivalent to Meduri et al. fig 8. [11].

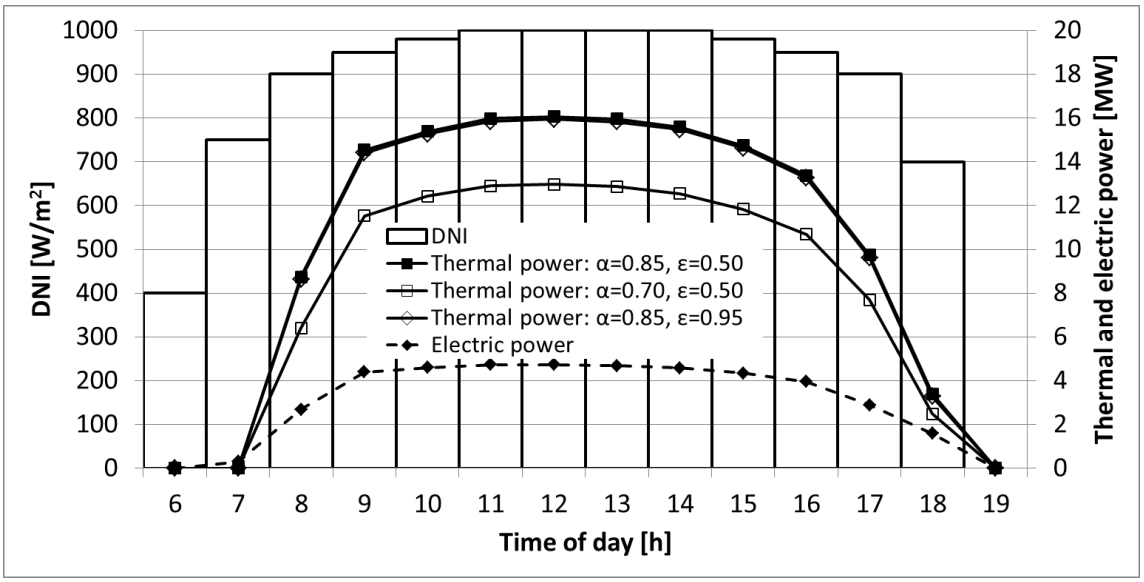

Fig. 4. Simplified model of thermal and electric power

Results for thermal power show good agreement with both simulated and measured data from Meduri et al. at about 16 MW_{th} at noon. The model predicts a similar slower start in the morning to measured results due to setting a lumped capacitance (inertia) based on commonly known startup times of CSP plants. A sensitivity test showed a high degree of sensitivity to solar absorptivity and a low sensitivity to thermal emissivity. Electrical power was determined but due to the elementary formulation and the difference between the architecturally rated and measured performance of this plant, these results are not discussed.

5. Conclusion and further work

This work represents a small component of a larger project that requires specific attention due to the complicated nature of a central receiver CSP plant. The method determines the power delivery of a central receiver plant almost instantaneously based on typical mean year data. Initial validation suggests that the method is more than suitable for the task of conducting analysis on a regional basis and to provide decision makers with a quick method to assess CSP technology.

Further validation is required to test different central receiver plant variants. A more accurate manner to determine electrical power is required. Once these improvements are made, the other three CSP plant types will be modeled using similar methods in order to create a basis for comparison between types. Parameters such as cost, water use, storage and backup fuel are all currently under development in the model.

Acknowledgements

The authors would like to thank Sasol Technology, the Department of Science and Technology of South Africa through the Solar thermal spoke fund and the Stellenbosch University Hope project for funding the resources to perform this work and present it at SolarPACES. The advice and support of Professor Wikus van Niekerk of the Centre for Renewable and Sustainable Energy Studies, Emeritus Professor Detlev Kröger and Dr. Hanno Reuter of the Mechanical and Mechatronic Engineering department is also appreciated.

References

[1] M. Edkins, H. Winkler, A. Marquard, (2009), Large Scale Rollout of Concentrating Solar Power in South Africa, Energy Research Centre, University of Cape Town, Cape Town.

[2] International Energy Agency (IEA), (2010), Technology Roadmap – Concentrating Solar Power. OECD/IEA, Paris.

[3] A.C. Brent, T. Pretorius, (2010), Solar Energy Technology Roadmap of South Africa, DST SETRM 2010

[4] Thomas P. Fluri, (2009), The potential of concentrating solar power in South Africa, Energy Policy, Vol. 37, pp. 5075-5080.

[5] Torresol Energy, (2011), Gemasolar solar power plant reaches 24 hours of uninterrupted production, Company website, http://www.torresolenergy.com/TORRESOL/NewsTS/gemasolar-solar-power-plant-reaches-24-hours-of-uninterrupted-production, accessed 16 July 2011.

[6] Business Day, (2011), EDITORIAL: Delay hampers green power, Business Day website, http://www.businessday.co.za/articles/Content.aspx?id=147450, accessed 16 July 2011.

[7] Terence Creamer, (2011), Surging tariffs and interest bill, but also signs of greater stability at Eskom, Engineering news online, Creamer media, http://www.engineeringnews.co.za/article/eskoms-interest-bill-surging-but-funding-plan-advanced-2011-07-08, accessed 15 July 2011.

[8] Republic of South Africa, Department of Energy, (2011), Electricity Regulation on the Integrated Resource Plan 2010 – 2030, Government gazette, No. 34263.

[9] S. Schell, (2010), Design and evaluation of eSolar's heliostat fields, Solar Energy.

[10] S. Schell, (2010), Personal communication.

[11] Phani K. Meduri et al., (2010), Performance characterization and operation of eSolar's Sierra SunTower power tower plant, SolarPACES 2010.

[12] National Renewable Energy Laboratory (NREL), National Solar Radiation Data Base, 1991- 2005 Update: Typical Meteorological Year 3, NREL, http://rredc.nrel.gov/solar/old_data/nsrdb/1991-2005/tmy3/by_state_and_city.html#C, accessed 26 July 2011.

[13] National Renewable Energy Laboratory (NREL), (2011), Sierra SunTower project overview, NREL/SolarPACES, http://www.nrel.gov/csp/solarpaces/project_detail.cfm/projectID=63, accessed 27 July 2011.